MODELING THE EFFECTS OF TEMPERATURE FEEDBACKS ON SELF-ORGANIZED VEGETATION PATTERNS IN SEMI-ARID GRASSLANDS

A THESIS

Presented To

The Faculty of the Department of Environmental Science

The Colorado College

In Partial Fulfillment of the Requirements for the Degree

Bachelor of Arts

By

Ewan Y. Henderson

May 2024

Dr. Miroslav Kummel
Associate Professor of Environmental Science

Dr. David Brown
Associate Professor of Mathematics and Computer Science

Table of Contents

Abstract

Self-organized periodic vegetation patterns in arid grasslands are thought to originate from a local positive feedback whereby vegetation density increases infiltration coupled with a long-distance negative feedback whereby vegetation patches deplete water from surrounding areas, leaving these bare. Studies show that this patterning could indicate approaching catastrophic ecosystem collapse. Previous models have described the dynamics of vegetation coupled with soil and surface water. However, several other positive feedbacks may occur, including one between vegetation density and local surface temperature. At our field site, it was observed that surface temperatures are cooler in vegetation patches (~35ºC) and hotter in areas of bare ground (>50ºC) due to evapotranspiration. This feedback indicates that the presence of vegetation further supports plant growth by cooling the surface to a temperature suitable for vegetation growth and has not been previously modeled or studied for its impact on vegetation pattern formation. This study analyzes the effect of adding the temperature feedback to the HilleRisLambers model on vegetation patterning. To do this, we multiplied the vegetation growth term by a temperature-dependent term P/(h+P) where P represents plant density and h determines the model's temperature dependence. We then ran the model at different h values and levels of rainfall to understand how the dynamics of the model were changed by this modification.

The simulations run with our modified model indicate a temperature feedback might affect vegetation patterning. The inclusion of a temperature feedback appears to widen the area of bistability when vegetation biomass (P.mean) is plotted against rainfall (R). Without the temperature feedback (h=0), the area of bistability is within the range of R=0.875 and R=0.995. Including the temperature feedback (h=0.05), this range became from R=0.9375 to R=1.5 and

expanded further as h increased. Our results created new questions about pattern formation approaching the catastrophic bifurcation switch point and at higher rainfall levels. Literature suggests that patterning increases as the system approaches desertification. While our model was able to recreate patterns observed in nature and in previous studies, specifically labyrinth and fairy rings, at higher values of h (and hence higher temperature dependence of plant growth), we also observed decreased patterning approaching catastrophic bifurcation, contradicting previous studies. Additionally, our model produced patterns resembling patterns formed in Belousov-Zhabotinsky reactions. While this has not been observed in previous studies or in nature, further exploration into the mathematics behind these results would be interesting.

Introduction

Mathematical modeling has been a useful tool in understanding the behavior of self-organized vegetation patterning in arid ecosystems. Multiple studies have developed models that study the positive feedback between infiltration and plant density as a mechanism responsible for vegetation patterning. While this process has been established as likely the primary driver for patterning, our study explores the impact of a second additional positive feedback existing in the system. Building upon previous models, our study includes an additional positive feedback which correlates cooler local air temperature with greater plant density. This paper will discuss how we included the temperature feedback in the model and compares its results to previous studies.

Vegetation Patterning and Mechanisms:

Self-organized vegetation patterning has been observed in arid ecosystem throughout the world (Rietkerk et al., 2002; Bromley et al., 1997; HilleRisLambers et al. 2001). Patterns

observed in nature are uniform vegetation, gaps ("fairy rings"), stripes ("labyrinth" or "tiger bush"), spots, and uniform bare soil (Rietkerk et al., 2002; Getzin et al., 2021; Zelnik et al., 2013). Stipes and gaps have been observed and studied at Chico Basin Ranch, in Southwestern Colorado. The temperature feedback was observed by Cross et al. (2022) at this site, thus making this site the inspirational framing for our model.

There have been a range of hypothesized mechanisms responsible for this vegetation pattern formation, but the most accepted mechanism is a positive feedback between vegetation density and water infiltration (HilleRisLambers et al. 2001; Klausmeier et al., 1999; Bromley et al., 1997; Zelnik et al., 2013). This is coupled with long-distance negative feedback whereby vegetation patches deplete water from surrounding areas through long-range facilitation dependent on advection and diffusion (Rietkerk et al., 2004). In advection dominate systems, hillslope causes water to flow over areas of bare ground that are more impermeable and accumulate in vegetated patches where infiltration rates are heightened. Water is also redistributed through diffusion, where higher film heights of surface water will flow over to areas of lower film heights of surface water. In this feedback, patches of vegetation accumulate water through advection, as bare patches will not absorb precipitation and instead causing it run off and flow into patches of vegetation. Surface water diffusion also occurs, where vegetation patches retain surface water at a lower water column due to a greater infiltration rate, attracting water flow from higher water columns over bare patches. This water accumulates in patches of higher vegetation density, where the water infiltrates into the soil at a greater rate (HilleRisLambers et al. 2001). This results in higher levels of soil moisture in vegetated patches, which supports further vegetation growth in these patches (Klausmeier et al., 1999). The combination of the short and long range feedbacks has been identified as the primary mechanisms for vegetation

self-organization in arid grasslands, and necessary for pattern formation (HilleRisLambers et al., 2001; Rietkerk et al., 2004).

Bistability and Early Warning Signs:

The formation of patterning in arid grasslands can be attributed to the presence of local bistability. The alternation of grass patches and bare patches and the result of the existence of two stable states in this system. This is the local bistability that is created by positive feedbacks which supports vegetation growth in areas of dense vegetation and hinders growth in areas of bare soil (Cross et al., 2022). These stable states perpetuate the existence of each other, as vegetation thrives in areas of dense vegetation, but vegetation growth in hindered in areas of bare soil.

This causes a threshold vegetation population at which the population cannot establish below, called an Allee point (Cross et al., 2022). This is a switch point in the system at which any population above the point will be able to establish and thrive, where as any population below this point will be unable to establish and experience desertification. This is the bistability caused by positive feedback loops which determine the population trajectory in this system (Edelstein-Keshet, 1998). In systems such as this one, there exist a region of bistability where conditions are such that stable population and catastrophic population collapse are both possible depending on the initial population in the system. The values at which the initial population must be above to sustain a stable population at these conditions are Allee points, and these points make up the dashed line shown in Figure 1 taken from Rietkerk et al. (2004). This line divides the area of global bistability, above it the population will be able to establish and below it the population will crash. This figure also shows where the points of catastrophic bifurcation exist at the end points of the two solid lines. These points are at the lowest rainfall capable of supporting

population establishment and the highest rainfall at which the population can crash, and together these points make up the boundaries of the area of bistability.

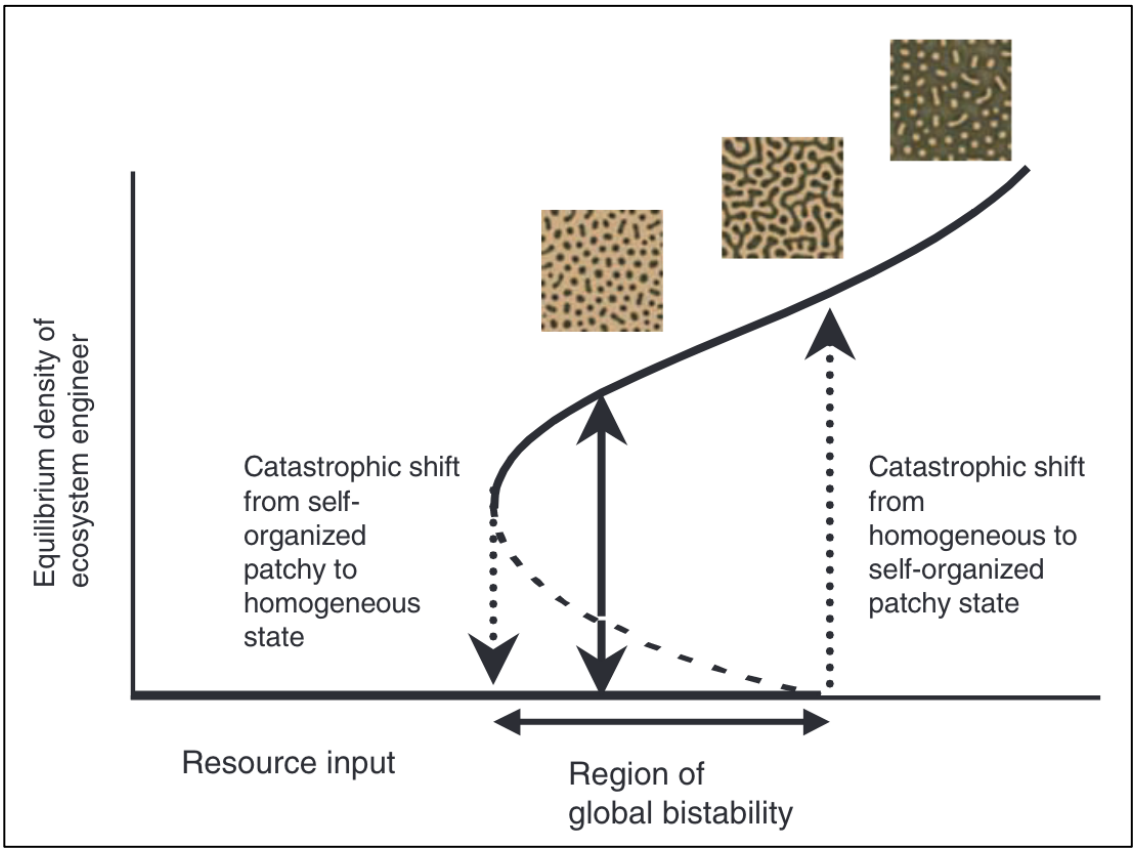

Figure 1: This figure taken from Rietkerk et al. (2004) shows how patterning changes with the changes in population as resource input (rainfall) increase or decreases. The solid lines represent mean equilibrium densities of consumers functioning as ecosystem engineers. Dotted arrows represent catastrophic shifts between self-organized patchy and homogeneous states, and vice versa. Dark colors in the insets represent high density. The range of resource input for which global bistability and hysteresis exists is between these dotted arrows. Solid arrows represent development of the system toward the coexisting self-organized patchy state or homogeneous state, depending on initial ecosystem engineer densities. (Rietkerk et al., 2004)

Pattern formation has been identified as a potential early warning sign of approaching desertification (Kéfi et al., 2014). It has been observed in previous literature that patterning rates increase as the system approaches catastrophic ecosystem collapse (Rietkerk et al. 2004). As

rainfall level decrease in systems where overland flow is dominated by advection, vegetation pattern wavelength increases until reaching uniform bare soil and desertification (Rietkerk et al. 2004; Dakos et al. 2011). In systems where overland flow is dominated by diffusion spots appear and increase in number as rainfall decrease until the system eventually reaches desertification (Dakos et al. 2011). If patterning is an indicator of approaching ecosystem collapse, understanding this behavior is essential for predicting the trajectory of these systems with the changing climatic conditions. Arid grasslands globally are seeing climate trends of decreased rainfall and hotter temperatures. Understanding how these changes will impact vegetation growth is important to local economies which rely on the success of grazing livestock.

Modeling Pattern Formation:

Previous studies have developed models to predict the pattern formation behavior as a consequence of this positive feedback between vegetation biomass and infiltration rate using partial differential equations (Klausmeier et al., 1999; HilleRisLambers et al. 2001; Rietkerk et al., 2002; Liu et al. 2022). Our model built upon the model first developed by HilleRisLambers et al. (2001) and Rietkerk et al. (2002). This model is a set of three partial differential equations, which describe the dynamics of plant density (P; g m^{-2}), soil water (W; mm), and surface water (O; mm). In the plant density equation, plant growth is dependent on plant density and soil water content, as a greater density of plants increases infiltration. The infiltration term's plant density dependence represents the positive feedback loop and is present in all three equations. This equation also accounts for plant mortality and dispersal to calculate for plant density. The soil water is positively dependent on infiltration and negatively dependent on uptake by plants. Both of these processes are dependent on plant density. Additionally, the soil water equation accounts

for evaporation, drainage, and dispersal. Lastly, the ground water equation has rainfall as the positive input and infiltration and dispersal as negative terms.

Our model builds on this model by including a second feedback between vegetation density and air temperature to the system. This is an additional positive feedback found by Cross et al. (2022) that correlates locally higher Normalized Difference Vegetation Index (NDVI) with locally cooler temperature, and locally lower NDVI with locally hotter temperatures. This study found that bare areas were approximately 4.8ºC hotter than areas of denser vegetation (Cross et al., 2022). Importantly, the hotter temperatures measured in bare areas (~48.4ºC) were too hot for vegetation to grow, whereas the cooler temperatures measured in vegetated patches (~43.6ºC) were just below the upper limit of vegetation's growable temperature range (Cross et al., 2022). These temperatures were found in patches of vegetation and bare soil located only a few centimeters apart, indicating this differential is extremely localized (Cross et al., 2022). This temperature differential is likely due to evapotranspiration (ET) from vegetation cooling local air temperature (Cross et al., 2022; Dunkerly et al. 2018). Increased infiltration in densely vegetated areas would increase ET, support plant growth by cooling local air temperature (Dunkerly et al. 2018). Existing conceptual mathematical models have not explored the influence of ET and air temperature on pattern formation. Our study modifies existing models to include the presence of a temperature feedback in the system and analyzes how this inclusion changes the dynamics and pattern formation.

To include the temperature feedback in our model, we created a temperature dependence term which me multiplied with our growth term in our vegetation biomass equation. We defined this term as $\frac{P}{h+P}$, where we created a new variable h to determine the influence of temperature on the system. This term was multiplied to the plant growth term in our plant density equation. This

means that at h=0 and high values of P, the growth rate would be the same as the original model. When h has value and is not sufficiently smaller than R, the growth rate will be a fraction of the maximal rate. This represents the hinderance of growth caused by increased temperature present in areas of bare soil and the supported growth in areas of dense vegetation.

To analyze the effects of the temperature feedback on the system and the vegetation pattern formation, we ran the model at different values of temperature dependence (h) and precipitation (R). We also ran the model at differing initial conditions of vegetation biomass to create a catastrophic bifurcation plot and understand the region of bistability for different values of h. In this paper, we will compare the results of our model to the results of similar model that do not include the temperature feedback to understand the effect of this mechanism and how it is changing the system.

Purpose of this Study:

The goal of this study was to create a model which built upon previous self-organized vegetation patterning models by including an additional positive feedback loop. Previous studies have modeled the infiltration and plant density feedback that has been attributed as the primary mechanism for vegetation patterning. Our model introduces a local temperature and plant density positive feedback that could be an additional mechanism for patterning. This feedback was observed at Chico Basin Ranch by Cross et al. (2022) and has not previously been modeled or studied for its effect of patterning. This temperature feedback could further facilitate patterning though supported plant growth in areas of dense vegetation due to cooler local air temperature caused by evapotranspiration. This paper discusses the finding of our model and compares it to the findings of previous studies and literature that have used similar models that did not include the temperature feedback.

Methods

Model Development and Description:

Our model modified the model developed originally by HillesRisLambers et al. (2001), using the parameters used by Rietkerk et al. (2004) in their adoption of the model. This model was translated into code in RStudio by Liu et al. (2022). The model uses three partial differential equations to represent the infiltration feedback and water redistribution. The three equations describe the dynamics of plant density (P; g m^{-2}), soil water (W; mm), and surface water (O; mm). Parameters for the set of equations are defined in Table 1. The original model reads:

$$\textbf{EQ1}: \frac{\partial P}{\partial t} = c \times g_{max} \times \frac{W}{W + k_1} \times P - d \times P + D_P \Delta P,$$

$$\textbf{EQ2}: \frac{\partial W}{\partial t} = \alpha \times O \frac{P + k_2 \times W_0}{P + k_2} - g_{max} \times \frac{W}{W + k_1} \times P - r_w \times W + D_W \Delta W,$$

$$\textbf{EQ3}: \frac{\partial O}{\partial t} = R - \alpha \times O \frac{P + k_2 \times W_O}{P + k_2} + D_O \Delta O$$

EQ1 gives the plant density in (g/m^2) at a given location. This equation is made up by a plant growth rate term ($c \times g_{max} \times \frac{W}{W+k_1} \times P$), and plant death rate term ($d \times P$), and lastly a plant dispersal term ($D_P \Delta P$). In the plant growth rate term, ($g_{max} \times \frac{W}{W+k_1}$) gives the per capita water uptake. This rate is dependent on the amount of ground water in the system (W), as the greater W is, the closer this term will be the maximal per captia rate of uptake (g_{max}). The growth rate then depends on density of plants in the system (P). The term, ($g_{max} \times \frac{W}{W+k_1} \times P$) gives the uptake of ground water by plants, and this is converted into plant growth by c. The death rate term is also dependent on plant density, as d gives the per captia death rate of plants. Lastly, the plant dispersal term is added to represent plant reproduction. This term multiplies plant dispersal (D_p) by the change in plant density (ΔP).

EQ2 gives the soil water present in the system. This is determined by an infiltration term ($\alpha \times O\frac{P+k_2\times W_0}{P+k_2}$), a water uptake by plants term ($g_{max} \times \frac{W}{W+k_1} \times P$), an evaporation and drainage term ($r_w \times W$), and a soil water dispersal term ($D_W \Delta W$). The infiltration term is a function of plant density, where greater plant density increases infiltration by causing the term ($\frac{P+k_2\times W_0}{P+k_2}$) to approach 1 from W_0 at low plant density. This means at high plant densities; the infiltration rate will be near the maximal rate (α). The water uptake by plant term ($g_{max} \times \frac{W}{W+k_1} \times P$) is taken from EQ1 but is made negative here as plant uptake decrease soil water. The evaporation and drainage term is also negative, as it represents removal of ground water from the system at the rate of specific soil water loss due to evaporation and drainage (r_w) multiplied by the soil water content (W). Lastly, the soil water dispersal term is added to the system and is determined by the product of the diffusion coefficient for soil water (D_w) and the change in soil water content (ΔW).

The final equation, EQ3, determines the surface water content. This value is determined by rainfall (R), the infiltration rate ($\alpha \times O\frac{P+k_2\times W_O}{P+k_2}$), and surface water dispersal ($D_O \Delta O$). In this equation, precipitation is the positive input to the system and is determined by the variable R. Subtracted from this is the same infiltration term found in EQ2, representing the flow of surface water becoming ground water. Lastly, surface water dispersal representing overland flow of water is determined by the product of diffusion coefficient of surface water (D_0) and the change in surface water (ΔO)

To build in the additional positive feedback found by Cross et al. (2022), we created a new temperature dependence term. We defined this as $\frac{\mathrm{P}}{\mathrm{h+P}}$, where we created a new variable h to determine the influence of temperature on the system. This new term behaves as a type II

functional response that varies between 0 and 1. We included this term in out plant density equation (EQ1) by multiplying it into our plant growth term in that equation. This means the original growth rate will be the maximum growth rate and is only achieved when $\frac{\mathrm{P}}{\mathrm{h+P}}$ is equal to 1. This achieved when either h=0 or P is substantially greater than h. This behavior of this term allowed us to manipulate the dependence of plant growth by varying the value of h. With a larger h value, a higher plant biomass will be needed to bring the term to 1, whereas smaller h values will require less plant biomass to approach 1. This functions as the positive feedback observed in nature, where too few little vegetation will cause the growth rate to be a fraction of the maximal rate. Alternatively, denser vegetation will cause the growth rate to increase and approach the maximal rate as $\frac{\mathrm{P}}{\mathrm{h+P}}$ increases and approaches 1. The inclusion of the temperature dependence resulted in a modified set of equations:

Modified Model:

$$\mathbf{EQ4}: \frac{\partial P}{\partial t} = c \times g_{max} \times \frac{W}{W + k_1} \times P \times \frac{P}{h + P} - d \times P + D_P \Delta P,$$

$$\mathbf{EQ5}: \frac{\partial W}{\partial t} = \alpha \times O \frac{P + k_2 \times W_0}{P + k_2} - g_{max} \times \frac{W}{W + k_1} \times P - r_w \times W + D_W \Delta W,$$

$$\boldsymbol{EQ6}: \frac{\partial O}{\partial t} = R - \alpha \times O \frac{P + k_2 \times W_O}{P + k_2} + D_O \Delta O$$

In our modified model, the plant growth term is the only term changed. By multiplying this term by $\frac{P}{h+P}$, it means the plant growth will be decreased as *h* increases…

Table 1:

Symbol	Interpretation	Unit	Value (or Range)
P	Plant density	g/m^2	——
W	Soil water	mm	——
O	Surface water	mm	——
h	Temperature dependence term		0-1
R	rainfall	mm/d	0.75-2

c	conversion of water uptake by plant growth	$g*mm^{-}1*m^{-2}$	10
g_{max}	maximum specific water uptake	$mm*g^{-1}*m^2*d^{-1}$	0.05
k_1	half-saturation constant of specific plant growth and water uptake	mm	5
k_2	saturation constant of water infiltration	g/m^2	5
d	specific loss of plant density due to mortality	d^{-1}	0.25
W_0	water infiltration rate in the absence of plants	——	0.2
r_w	specific soil water loss due to evaporation and drainage	d^{-1}	0.2
D_p	is plant dispersal	m^2/d	0.1
D_w	diffusion coefficient for soil water	m^2/d	0.1
D_o	diffusion coefficient for surface water	m^2/d	100
α	Maximum infiltration rate	d^{-1}	0.2

Coding the Model:

We ran the model in RStudio using the "ReacTran" package. The array used in the model was a 100 by 100 array representing a 100m x 100m area. The array was initialized using a random draw from a uniform distribution between two numbers. We varied the boundaries of the uniform distribution to create our catastrophic bifurcation graph. The boundaries in out simulation were set to be closed and reflective boundaries. We also did not include advection, so our simulations represent a flat surface. We then ran the simulation for the time equivalent 3000 days. We did have a larger model that was a 200 by 200 array and ran for 5000 days. The two models gave qualitatively the same results in patterns produced, but the smaller model required significantly less time per simulation making it easier to work with. For these reasons, in this paper, we focused on only the results produced by smaller models. Although further exploration with the larger model could be done to explore how patterning behavior may change as the runtime continues. For each simulation, images of vegetation, ground water, and surface water distribution at the final day were recorded. Additionally, we took note of the h and R values set as the precondition, as well as the resulting mean P value (P.mean) in the final days array.

Experimentation with the Model:

To experiment with the model, we ran the model at various values of h and R to see how the patterning changed with increasing dependence on the temperature feedback and at different rainfall values. We ran simulations with h values ranging from h=0 (original model) to h=1. Our R values ranged from R=0.75 to R=2. In the unmodified version of the model (h=0), these R values were the boundaries of patterning, producing uniform bare and uniform grass cover respectively. We also varied the initial plant biomass to create our catastrophic bifurcation graph. To do this, we had three different ranges of plant density values where each pixel in our initial array was a randomly select value within this range. Our three ranges were (0-5), (0-20), and (0-50). This gave us simulations with the initial conditions used in Liu et al. (2022), as well as simulations with low and high initial plant biomass.

Results

To analyze the model, we ran it at various values of rainfall (R), temperature dependence (h), and initial biomass conditions. From these simulations, we were able to determine the effect of the added temperature dependence to the model. For each run we recorded the average value of P in the grid at the end of the run and the figure produced at the final timestep showing the vegetation patterning.

Correlation of h and R to biomass:

To study the relationship between h and R, we plotted the mean biomass of our simulations against increasing R values when h was kept constant. We did this at three values of h to see how the graph would change with increased temperature dependence.

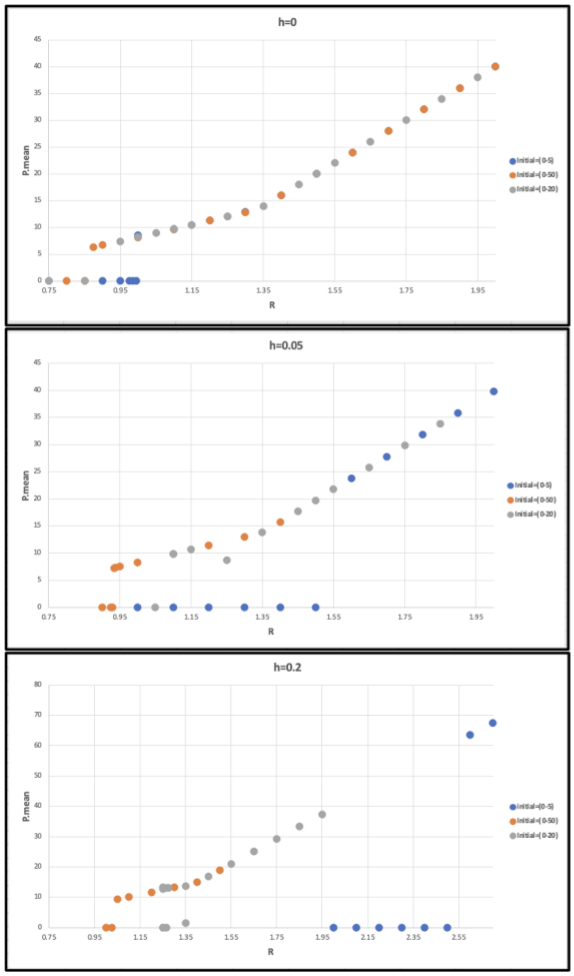

Figure 2: Spatial vegetation mean biomass (P.mean) with increasing rainfall (R) and varying influence from temperature feedback (h). Graph *A* has no influence from the temperature feedback (h=0). Graph *B* and *C* show as increased area of bistability as the h value increases (0.05 and 0.2 respectively) and the influence of the temperature feedback in increased.

In Figure 2, we observed increased mean biomass as the amount of rainfall increased with a constant h value. Additionally, we observed overall decreased biomass as we increased the h value at a constant rainfall. This is because high rainfall and low effect from temperature would positively impact the growth term in our plant growth equation. For constant h, we found the R value at which the population of vegetation would go to extinction. This switch point occurred at higher values of R (greater rainfall) as h increased. Along with this, higher values of h also appeared to have expanded the area of bistability. Figure 2 show that with no temperature influence (h=0), the region of bistability is at a lower R value and confined to a smaller range than those of our simulations with added heat influence. With the addition of the temperature feedback, simulations where the initial biomass levels were low resulted in desertification until

higher rainfall values. The figures reflect that with temperature dependence, even at high rainfall values there is potential for desertification if initial conditions of biomass are too low. This is not observed without the temperature feedback. With the h value set to 0, the lowest initial biomass conditions result in a stable vegetation biomass with relatively low rainfall values.

Observed in all three graphs is a kink in increased slope in around R=1.35. The plant biomass is always increasing, but at this threshold it appears to accelerate the rate at which it is increasing. Without the inclusion of the temperature feedback, the area of bistability is contained to an area below this kink (R<1.35), but in both graphs where h has a positive value the area of bistability expands past this kink. This means that beyond this point of increased slope, the system is still susceptible to desertification when the temperature feedback is added.

Patterning:

We plotted to resulting pattern figures with axes of R and h to understand how these variables effected the vegetation patterning behavior. We did this for each of the three initialization conditions we used. Generally, the ground water and surface water figures had similar patterns to the vegetation figures, so we have only included the vegetation patterns here.

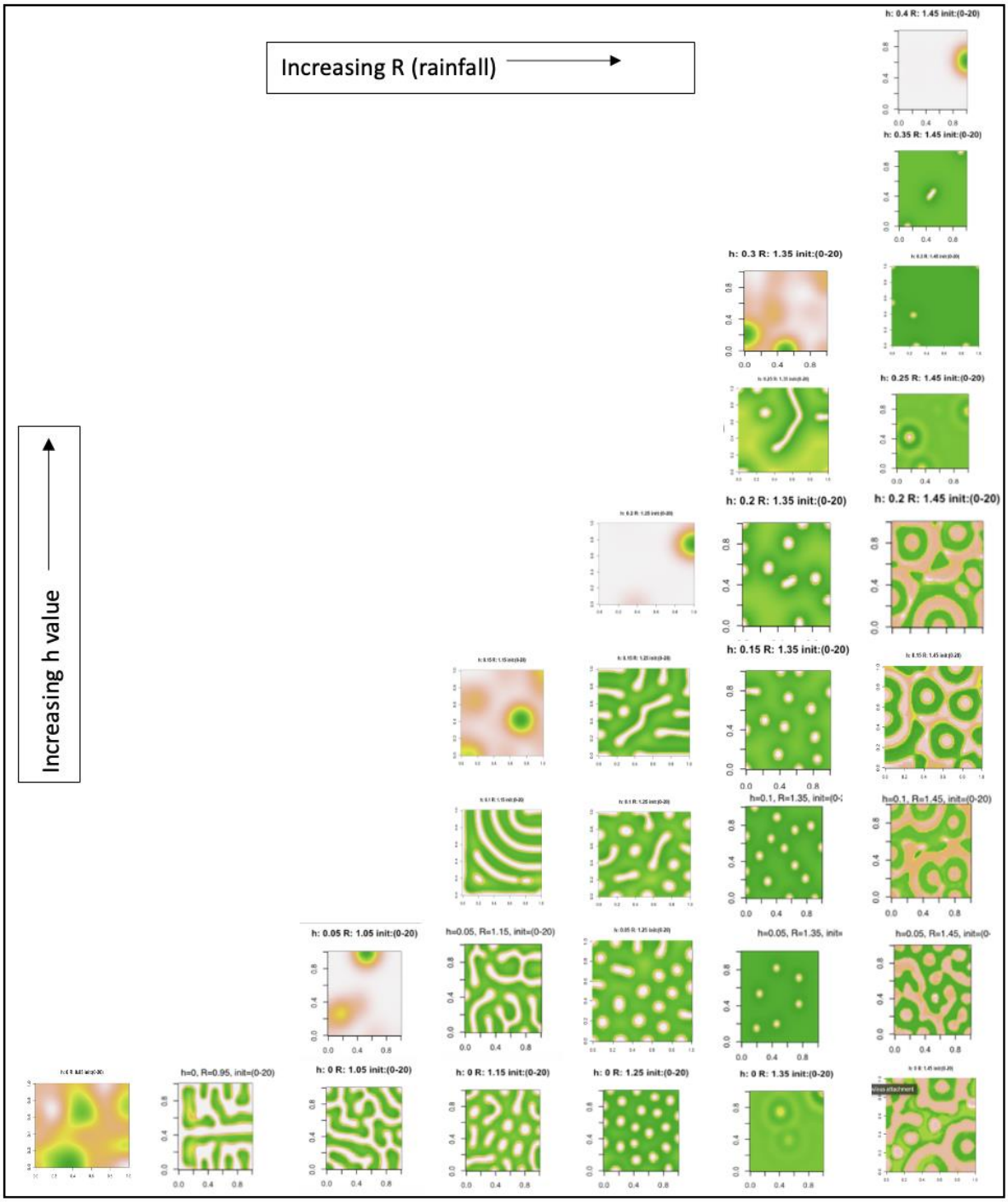

Figure 3: Changes to the vegetation patterns as rainfall (x axis) and temperature feedback influence (y axis) increase with range of initial biomass values set to (0-20). As rainfall increases, the spacing between vegetation patches decreases until it reaches uniform grass cover, but pattern then appear to form after this. Higher rainfall requires higher h values to result in desertification. As h increases and approaches desertification, patterning of the vegetation changes and appears to become more uniform.

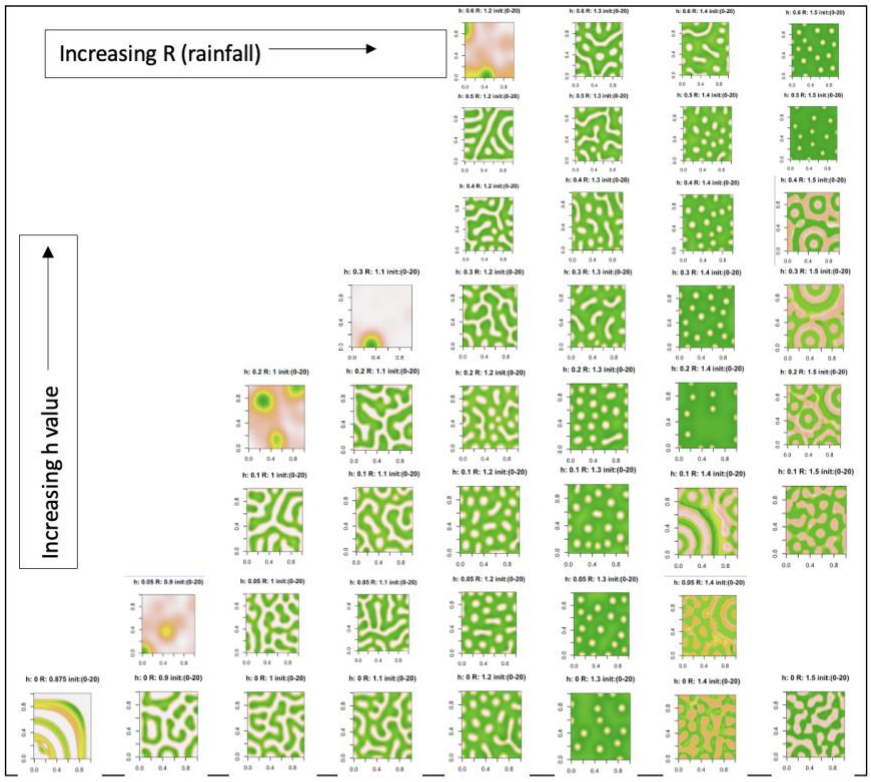

Figure 4: Changes to the vegetation patterns as rainfall (x axis) and temperature feedback influence (y axis) increase with range of initial biomass values set to (0-50). The increased vegetation preconditions result in longer survival of stable vegetation populations at higher values of h. The higher values of rainfall still create BZ patterns, but as temperature feedback increases, they revert to fairy rings. This appears to contradict the increased wavelength in patterning observed with higher values of h and decreased rainfall.

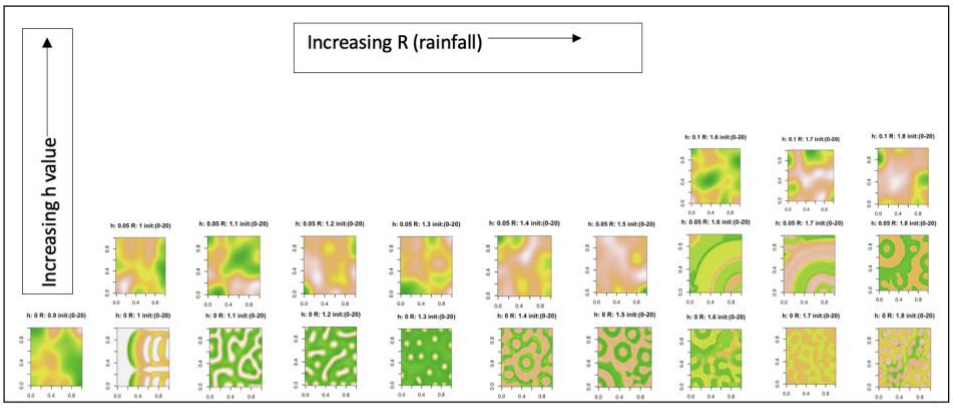

Figure 5: Changes to the vegetation patterns as rainfall (x axis) and temperature feedback influence (y axis) increase with range of initial biomass values set to (0-5). The lower initialization range produced much drier conditions. With the inclusion of the temperature feedback, much higher rainfall was required for the population to establish than under the previous conditions. Without the temperature feedback (h=0), the patterning behaved similarly to the other initial conditions.

We were able to replicate patterns found in other studies that have used versions of the Klausmeier model without temperature feedback. Specifically, we were able to produce labyrinth and fairy ring patterns at multiple values of h. These patterns have been observed commonly in nature and reproduced by models in multiple studies. When our model was run with no temperature influence (h=0), the sequence of patterning was similar to that found in other studies. Beginning at the lowest rainfalls and increasing, the patterning sequence order goes uniform bare soil, spots, stripes (labyrinth), gaps (fairy rings), and lastly uniform vegetation cover. This sequence indicates that patterning increase as water become more limited in the system. Due to the added temperature feedback, our model required a higher rainfall constant than used in the Liu et al. (2022) and Rietkerk et al. (2002) models to produce the same patterns. This meant the same patterns were observed but found at higher rainfall as h increased.

We also produced some patterns that have not been observed in previous studies. At higher rainfall values, the simulation produced patterns that we recognized as being similar the patterns created by Belousov-Zhabotinsky (BZ) reaction. This pattern can be seen in Figures 3,4 ad 5 at R=1.4 and greater. While the ring pattern we found look similar to these patterns formed in these chemical reactions, there is no movement of the pattern as observed in BZ reaction. The biomass mean values appears to become constant when these patterns appear, with the same P.mean value exactly repeating. Other patterns show dampened oscillation around an equilibrium P.mean value, but does become constant on one exact value.

Another new observation in our model was the pattern behavior around the point of catastrophic bifurcation. Two behaviors were observed at values of h and R near the switch point: uniform grassland or rippled pattern. This is best shown in Figure 3, specifically at R=1.15, R=1.35, and R=1.45. These patterns appear while the biomass is still decreasing as

approaching the catastrophic bifurcation point. At R=1.15, as h increases, the patterning transitions from labyrinth to arcing, parallel line that resemble a ripple immediately before the population collapses. At R=1.35 and R=1.45, the patterning begins as fairy rings, but increasing h causes the number of fairy rings to decrease approaching uniform vegetation cover. Patterning appears to stop at the h value just before the transition to population collapse and uniform bare soil overtakes the system.

Discussion

In this study, we modified periodic vegetation patterning models developed by HillesRisLambers et al. (2001) and Rietkerk et al. (2004) by including an additional positive feedback loop. Previous models had accounted for a positive relationship between infiltration rate and vegetation density, resulting in improved growth conditions in areas of dense vegetation and worsened growth conditions in bare areas. While this has been attributed as the primary mechanism for self-organized vegetation patterning, other mechanisms have been identified as potentially impactful, including a second positive feedback loop correlating local air temperature to vegetation cover found by Cross et al. (2022). Our model modifies previous models to include this temperature dependence feedback to understand how this feedback effects the system and patterning behavior. Our model reproduced some similar results that have been found in previous spatial vegetation patterning studies but has also produced results that contradict previous conclusions or has not been mentioned in previous literature.

The expanded region of bistability was only found with the inclusion of a temperature feedback. Previous studies have used a similar model and plotted the mean vegetation biomass with increasing rainfall as we did here. In these studies, the graphs produced show a similar curve and area of bistability as our graph with no temperature feedback (h=0) (Dakos et al.

2011). Once our model included the temperature feedback, the area of bistability widened significantly. The general shape of the graph was maintained, with a linear increase in the mean biomass with a kink and increase in slope. This area of bistability continued to increase as the h value increased in the model. An increased area of bistabilty has important implication for the conditions at which the system is vulnerable to collapse. The widened region indicates that even at higher rainfalls, the system could collapse if the population drops below the allee point.

The expanded area of bistability indicates that with the inclusion of a temperature feedback, the system remains vulnerable to desertification even at higher levels of rainfall if the initial conditions of vegetation biomass are low enough. This would change the understanding how susceptible arid grassland are to desertification, even at higher levels of rainfall. This indicates there is a greater region of rainfall at which vegetation biomass needs remains at a high enough value to avoid crossing the critical point. To fully understand the region of bistability, more simulations of the model would be needed to create more data points. This would need to be done at more values of h to understand how the influence of temperature causes this region to change.

Our results also contradict some of the previously observed patterning behaviors in similar models without the temperature feedback. Across multiple studies, it has been concluded that lower rainfall conditions resulted in patterns with larger wavelength (Rietkerk et al. 2004). The observed behavior has been, as aridity increases, from uniform vegetation cover to fairy rings, labyrinth, spots, and then bare soil (Deblauwe et al. 2011). Our results have shown this pattern at lower rainfalls, but our model does not reach uniform vegetation cover at higher rainfalls. At an R value around 1.4, patterns resembling BZ reactions begin to appear. Once formed, these patterns remain constant in form and P.mean value as time continues forward.

The R value of 1.4 is located just beyond the of the kink in our graph of R vs P.mean at constant values of h found at R=1.35 (Figure 1). This kink is an increase in slope of our linearly increasing vegetation biomass as rainfall increases. This has been created in previous studies that have used models without temperature feedback (Dakos et al. 2011). In these studies, the kink in the graph has been identified as Turning instability point where the feedback switches to being strong enough for pattern formation (Dakos et al. 2011; HilleRisLambers et al. 2001). While these studies have found that at rainfalls beyond the kink there should be uniform grass cover, our results were showing patterning.

This could be the result of a couple factors. Firstly, the patterning at higher rainfalls is variation in amount of grass cover, not variation between bare ground and vegetation. At lower rainfalls, color variation distinguishes areas of bare soil from vegetation. The patterns formed at higher rainfalls are representing variation in amount of grass growing in different patches, but there are likely no bare soil patches. This could be observed as uniform grass cover depending on the sensitivity of the color pallet used to create the figures. This would explain the reason for the formation of BZ patterns with no temperature feedback (h=0).

Another factor could be the exclusion of advection from our model. This is an important difference in our model from previous studies. Advection plays an important role in water transport in these systems and would change the patterns formed in our model if included. Adding advection to our current model would be relatively simple, but the analysis would be beyond the timeframe we have for the project at the moment and is the reason it was excluded here. This would be an interesting and logical next step for future work on this model.

Another finding of our model that contradicts previous literature is the behavior of patterning approaching catastrophic bifurcation. Previous papers have found that patterning

increases as vegetation approaches the catastrophic switch point and in the region of bistability (Rietkerk et al. 2004). This follows the sequence of self-organized patchiness as rainfall decrease and the patterns increase wavelength and patchiness until desertification (Rietkerk et al. 2004; Dakos et al. 2011). This has led to the thought that increased patterning could act as an indicator of approaching desertification in a system. Previous models have shown, this increased patterning as rainfall decrease and the system approaches desertification (Rietkirk et al. 2002). In our model, we were able to reproduce this patterning behavior when temperature dependence was kept constant.

Our model did not follow this pattern sequence when h was increased, and R remained constant. With the changes made to our model, the behavior approaching desertification as temperature dependence increased appears to behave differently. Figure 1 shows that with an increasing h value, the patterning increases until reaching very close to the switch point of desertification. Instead of continuing to increase wavelength of patterning, the vegetation appears to trend towards uniform before desertification occurs. The mean biomass is still decreasing in the system as it gets closer to desertification, but the patterning appears more uniform. The lack of pattern contradicts previous literature that have found pattern formation to be an indicator of approaching desertification. These results suggest the contrary, and the absence of patterning as h increases seems to indicate desertification. further analysis of the model to reach a conclusion.

These results could have a similar explanation as the unexpected patterns found at higher rainfall values. The color pallet used for the figures could be unable to detect subtle patterning occurring as vegetation biomass is decreasing and approaching desertification. This is unlikely, as the color pallet used in out model, “terrain.color” generates a vector of contiguous colors. This should show subtleties in patterning because it is not fixed and will adjust differential in the

array. Additionally, the addition of advection could change the patterning in these simulations. While these explanations could change the images produced, it is unlikely to create patterns in our results. The color pallet used to create the figures was able to detect variation further away from the desertification switch point. This means that if it is unable to detect variation at these conditions, the patterning is still decreasing as the system is approaching catastrophic bifurcation. Thus, even if there is subtle patterning, this would not follow the previously understood sequence of patterning in these systems. The addition of advection is likely to change the patterning that appears and would require further study to analyze. But advection unlikely to increase the wavelength of the patterning as it approaches desertification, which has been the previously observed behavior.

The inclusion of a temperature feedback appears to have changed the dynamics of the system, resulting in changed patterning behavior. Patterning is specifically behaving differently at the extreme ends of the system: very high and low biomass. The change in patterning at very low biomasses and approaching desertification could be related to the increased region of bistability mentioned above. If the system is more vulnerable to desertification because of the temperature feedback, this may change the sequence which the patterns appear.

Conclusion

Our study explored how the inclusion of an additional feedback loop dependent on temperature would affect vegetation patterning and growth in arid grassland ecosystems. Our model found that the introduction of this feedback effected the stability of the system and changed the behavior of the patterning sequence. While the general plant growth trends of our catastrophic bifurcation graphs were similar when the temperature feedback, the area of bistability was greatly widened because of the new feedback. This result implies that systems

which have this feedback may be more vulnerable to desertification, even at high rainfalls. This would change the understanding of the stable conditions and the population thresholds required for vegetation to establish in arid systems.

Our results also focused on the vegetation patterning and how the patterning changes as temperature dependence and rainfall change. While our model replicated patterning results found in previous studies, it also produced patterns contradicting previous conclusions. The previously held notion that patterning transitions to uniform grass cover at high rainfalls was contradicted by the rippled patterns resembling BZ patterns that appear in our model when R surpasses the 1.45 value. Additionally, the use of patterning as an early warning of approaching desertification has been hypothesized in multiple papers, but our model seems to contradict as well. At multiple rainfall values, as the h value increases and the system approaches collapse, patterning appears to decrease and approach uniform grass cover just before reaching the switch point of collapse. The addition of the temperature feedback appears to have affected the stability and patterning sequence in our model. This indicates that in systems influenced by this feedback may behave differently than those with only the infiltration feedback loop, potentially changing our understanding of self-organized vegetation pattering in arid grasslands.

Comparison of previous studies to our results indicate more research can be done to look at how the addition of a temperature feedback is affecting this system and the patterning. Firstly, the addition of advection would allow for more directly comparable work to previous studies. This would be the next step in continuing to build on this model and better understand how the temperature feedback is changing its behavior. This would provide more similarities to previous models and allow for a more useful comparison to prior research. Another area that would require further analysis, is the mathematics behind the formation of the BZ patterns. We were

unable to determine why they appear and what it might indicate, but a more focused study may be able to better understand. While these patterns have not been observed in arid grassland ecosystems, it is a pattern observed in nature and could be an interesting connection to explore deeper. Similarly, the patterns and uniformity observed approaching the point of catastrophic bifurcation would an interesting exploration to understand that behavior.

References

Baudena, M., Fabio D'Andrea, and Antonello Provenzale. 2009. "A Model for Soil-Vegetation-Atmosphere Interactions in Water-Limited Ecosystems (Vol 44, Art No W12429, 2008)." *Water Resources Research* 45 (February). https://doi.org/10.1029/2008WR007694.

Baudena, M., Jost Hardenberg, and Antonello Provenzale. 2013. "Vegetation Patterns and Soil-Atmosphere Water Fluxes in Drylands." *Advances in Water Resources* 53 (March): 131–38. https://doi.org/10.1016/j.advwatres.2012.10.013.

Bromley, J., J. Brouwer, A. P. Barker, S. R. Gaze, and C. Valentine. 1997. "The Role of Surface Water Redistribution in an Area of Patterned Vegetation in a Semi-Arid Environment, South-West Niger." *Journal of Hydrology* 198 (1): 1–29. https://doi.org/10.1016/S0022-1694(96)03322-7.

Chen, Zheng, Jieyu Liu, Li Li, Yongping Wu, Guolin Feng, Zhonghua Qian, and Gui-Quan Sun. 2022. "Effects of Climate Change on Vegetation Patterns in Hulun Buir Grassland." *Physica A: Statistical Mechanics and Its Applications* 597 (July): 127275. https://doi.org/10.1016/j.physa.2022.127275.

Cross, Natalie, Miroslav Kummel, and Shane Heschel. 2022, "Perpetuating Bistability in the Self-Organized, Arid Grasslands of Southeastern Colorado: A Proposed Novel Feedback Driven by Evapotranspiration and Seasonality." [Unpublished undergraduate thesis]. Colorado College.

Dakos, Vasilis, Sonia Kéfi, Max Rietkerk, Egbert H. Van Nes, and Marten Scheffer. 2011. "Slowing Down in Spatially Patterned Ecosystems at the Brink of Collapse." *The American Naturalist* 177 (6): E153–66. https://doi.org/10.1086/659945.

Deblauwe, Vincent, Pierre Couteron, Olivier Lejeune, Jan Bogaert, and Nicolas Barbier. 2011. "Environmental Modulation of Self-organized Periodic Vegetation Patterns in Sudan." *Ecography* 34 (July): 990–1001. https://doi.org/10.1111/j.1600-0587.2010.06694.x.

D'Odorico, Paolo, Francesco Laio, and Luca Ridolfi. 2006. "Vegetation Patterns Induced by Random Climate Fluctuations." *Geophysical Research Letters* 33 (19). https://doi.org/10.1029/2006GL027499.

Dunkerley, David. 2018. "Banded Vegetation in Some Australian Semi-Arid Landscapes: 20 Years of Field Observations to Support the Development and Evaluation of Numerical Models of Vegetation Pattern Evolution," January.

Edelstein-Keshet, L. 1998. *Mathematical Models in Biology*. Random House.

Getzin, Stephan, Todd E. Erickson, Hezi Yizhaq, Miriam Muñoz-Rojas, Andreas Huth, and Kerstin Wiegand. 2021. "Bridging Ecology and Physics: Australian Fairy Circles Regenerate Following Model Assumptions on Ecohydrological Feedbacks." *Journal of Ecology* 109 (1): 399–416. https://doi.org/10.1111/1365-2745.13493.

HilleRisLambers, R., M. Rietkerk, F. van den Bosch, H. H. T. Prins, and H. de Kroon. 2001. "Vegetation Pattern Formation in Semi-Arid Grazing Systems." *Ecology* 82: 50–61. https://doi.org/10.1890/0012-9658(2001)082[0050:vpfisa]2.0.co;2.

Kéfi, Sonia, Vasilis Dakos, Marten Scheffer, Egbert H. Van Nes, and Max Rietkerk. 2013. "Early Warning Signals Also Precede Non-catastrophic Transitions." *Oikos* 122 (5): 641–48. https://doi.org/10.1111/j.1600-0706.2012.20838.x.

Kéfi, Sonia, Vishwesha Guttal, William A. Brock, Stephen R. Carpenter, Aaron M. Ellison, Valerie N. Livina, David A. Seekell, Marten Scheffer, Egbert H. Van Nes, and Vasilis Dakos. 2014.

"Early Warning Signals of Ecological Transitions: Methods for Spatial Patterns." Edited by Ricard V. Solé. *PLoS ONE* 9 (3): e92097. https://doi.org/10.1371/journal.pone.0092097.

Klausmeier, Christopher A. 1999. "Regular and Irregular Patterns in Semiarid Vegetation." *Science* 284 (5421): 1826–28. https://doi.org/10.1126/science.284.5421.1826.

Lefever, René, Nicolas Barbier, Pierre Couteron, and Olivier Lejeune. 2009. "Deeply Gapped Vegetation Patterns: On Crown/Root Allometry, Criticality and Desertification." *Journal of Theoretical Biology* 261 (2): 194–209. https://doi.org/10.1016/j.jtbi.2009.07.030.

Liu, Silvi and Miroslav Kummel. 2022. "Modeling self-organized periodic pattern in arid grasslands: Patterns askew to the slope develops when vegetation impedes sheet flow" [Unpublished undergraduate independent study]. Colorado College.

Meron, Ehud, Jamie J. R. Bennett, Cristian Fernandez-Oto, Omer Tzuk, Yuval R. Zelnik, and Gideon Grafi. 2019. "Continuum Modeling of Discrete Plant Communities: Why Does It Work and Why Is It Advantageous?" *Mathematics* 7 (10): 987. https://doi.org/10.3390/math7100987.

Rietkerk, Max, Maarten C. Boerlijst, Frank Van Langevelde, Reinier HilleRisLambers, Johan van De Koppel, Lalit Kumar, Herbert H. T. Prins, and André M. De Roos. 2002. "Self-Organization of Vegetation in Arid Ecosystems." *The American Naturalist* 160 (4): 524–30. https://doi.org/10.1086/342078.

Rietkerk, Max, Stefan C. Dekker, Peter C. De Ruiter, and Johan Van De Koppel. 2004. "Self-Organized Patchiness and Catastrophic Shifts in Ecosystems." *Science* 305 (5692): 1926–29. https://doi.org/10.1126/science.1101867.

Sticpewich, H. (2022). *Microhydrological soil and surface water movement in an emergent periodically patterned landscape at Chico Basin, CO.* [Unpublished undergraduate thesis]. Colorado College.

Valentin, C, and J. M d'Herbès. 1999. "Niger Tiger Bush as a Natural Water Harvesting System." *CATENA* 37 (1): 231–56. https://doi.org/10.1016/S0341-8162(98)00061-7.

Yariyan, Peyman, Mahdis Amiri, Maryam Saffariha, Mohammadtaghi Avand, Seid Saeid Ghiasi, and John P. Tiefenbacher. 2022. "Spatial Analysis of Environmental Factors Influencing Dust Sources in the East of Iran Using a New Active-Learning Approach." *Geocarto International* 37 (26): 11929–54. https://doi.org/10.1080/10106049.2022.2063393.

Zelnik, Yuval R., Shai Kinast, Hezi Yizhaq, Golan Bel, and Ehud Meron. 2013. "Regime Shifts in Models of Dryland Vegetation." *Philosophical Transactions of the Royal Society A: Mathematical, Physical and Engineering Sciences* 371 (2004): 20120358. https://doi.org/10.1098/rsta.2012.0358.

Zhabotinsky, Anatol M. 2007. "Belousov-Zhabotinsky Reaction." *Scholarpedia* 2 (9): 1435. https://doi.org/10.4249/scholarpedia.1435.

Acknowledgements

I want to thank Dr. Miro Kummel for his advising and support throughout this project. From coding and creating the model, to the drafting and editing this paper, Dr. Kummel was extremely helpful and supportive the entire way. I would also like to thank Dr. David Brown for reviewing and editing my drafts, as well as providing insight as I conducted my research. Thank you to the thesis/ice cream social crew: Sabine Blumenthal, Cole Pietsch, Jordan Cosgrove, and Olivia Gossett for the help and support throughout the research and writing process. Lastly, thank you to my friends and family for supporting me and putting up with me showing them all the pretty pictures I was making with my model!

Appendix

1. RStudio code for simulation of plant growth, and water redistribution on a flat surface with infiltration and temperature positive feedbacks:

```
library(ReacTran)

#setting up the grid
#400*400 meters, 200*200 elements
Nx<-100
Ny<-100
Grid.x<-setup.grid.1D(x.up=0,x.down = 200, N=Nx) #subdivided domain in x direction of 0 to 400 into 200 segments
Grid.y<-setup.grid.1D(x.up=0,x.down = 200, N=Ny)#subdivided domain in y direction of 0 to 400 into 200 segments ..
# please note that we combine the two grids inside the "function" for the whole system ... where the diferential functions are defined

#Defining the diffusion coefficients for plant spread and surface and ground water redistribution
D_P <- 0.1 # m^2/d
D_W <- 0.1# m^2/d
D_O <- 100 # m^2/d

#Parameters
c<-10 #conversion of water to plant biomass
g_max<-0.05 # max water uptake
k1<-5 #half saturation of water uptake
k2<-5 #saturation constant of the water infiltration
W0<-0.2 #water infiltration rate in the absence of plants
rw<-0.2 #specific soil water loss due to evap/drainage
a <-0.2 #max infiltration rate

#temperature dependence on growth
h<-0.3  #mess with this

#rainfall
R<-1.0 #mess with this
d <- 0.25 #ranges from 0 to .5, mortality #0.25 originally

#Some parameter values based on literature tested with h=0:
#R= 0.75 for spots... all plants are dead
#R= 1.0 Labyrinth....YES
#R= 1.25 Fairy rings/gaps ---OK
#R= 1.0 Bands with periodic boundary

#Defining the system of partial diffential equations
```

```
model1<-function(t,y,parms){
  P<-matrix(nrow=Nx,ncol=Ny,data=y[1:(Nx*Ny)])
  W<-matrix(nrow=Nx,ncol=Ny,data=y[(Nx*Ny+1):(2*Nx*Ny)])
  O<-matrix(nrow=Nx,ncol=Ny,data=y[(2*Nx*Ny+1):(3*Nx*Ny)])
  dP.dt<-c*g_max*(W/(W+k1))*P*(P/(h+P))-d*P+
    tran.2D(C=P, D.x=D_P, D.y=D_P, flux.x.up=0, flux.x.down=0, flux.y.up=0,flux.y.down=0,
dx=Grid.x, dy=Grid.y)$dC
  dW.dt<-a*O*((P+k2*W0)/(P+k2))-g_max*(W/(W+k1))*P-rw*W+
    tran.2D(C=W, D.x=D_W, D.y=D_W, flux.x.up=0, flux.x.down=0, flux.y.up=0,flux.y.down=0,
dx=Grid.x, dy=Grid.y)$dC
  dO.dt<-R-a*O*((P+k2*W0)/(P+k2))+
    tran.2D(C=O, D.x=D_O, D.y=D_O, flux.x.up=0, flux.x.down=0, flux.y.up=0,flux.y.down=0,
dx=Grid.x, dy=Grid.y)$dC
  list(c(dP.dt,dW.dt,dO.dt))
}
#Initial conditions:
P.ini<-matrix(nrow=Nx, ncol=Ny, data=runif(Nx*Ny,0,20)) #mess with this
W.ini<-matrix(nrow=Nx, ncol=Ny, data=runif(Nx*Ny))
O.ini<-matrix(nrow=Nx, ncol=Ny, data=runif(Nx*Ny))

y.ini<-c(P.ini,W.ini,O.ini)
#y.ini<-out.result
times<-seq(from=0, to=3000, by=1)
#Take 3000 times based on the paper: this model aims to be a replicate of the model that's being
implemented on the
#times<-seq(from=0, to=30000, by=100) # try this time step

# running the model
system.time(out<-ode.2D(y=y.ini, parms=NULL, times=times, func=model1, nspec=3,
dimens=c(Nx,Ny),
          lrw=1e8,names=c("P","W","O")))
#nspec: the number of the species in the model
#lrw: the length of the workspace

dim(out) #3001 30001
#Plant(P): 1:10000
#Soil water(W): 10001:20000
#Surface water(O): 20001:30000

#Result
out.2<-out[3000,]
out.result<-out.2[2:30001]
out.P<-out.result[1:10000]
out.W<-out.result[10001:20000]
out.O<-out.result[20001:30000]
mean(out.P)
```

```
h
R
a.P<-matrix(data=out.P,nrow=Nx,ncol=Ny)
image(a.P, col=rev(terrain.colors(30000)), main=paste("h:", h, "R:", R, "init:(0-20)"))
a.W<-matrix(data=out.W,nrow=Nx,ncol=Ny)
image(a.W, col=rev(topo.colors(12000)))
a.O<-matrix(data=out.O,nrow=Nx,ncol=Ny)
image(a.O, col=rev(topo.colors(12000)))
```

2. Site Description:

The site our model was based on is located near Hanover in El Paso County, Colorado at Chico Basin Ranch. The ecosystem at this site is an arid, high plains, shortgrass steppe where vegetation patterning has been observed and studied. At the site, the dominant grass species is blue grama (*Bouteloua gracilis*). Other plants found at the site include buffalograss (*Bouteloua dactyloides*), needle-and-thread (*Hesperostipa comata*), Russian thistle (*Kali tragus*), and cacti such as tree cholla (*Cylindropuntia imbricata*) and plains prickly pear (*Opuntia polyacantha*) (Cross et al., 2022). The 30-year annual average precipitation in this area is 12.04 inches, with monthly average precipitation peaking in August at 2.11 inches. The average temperature at the site is 74.8ºF, with a minimum temperature of 59.4°F and a maximum temperature of 90.2°F (Pueblo NWS).

Periodic patterns containing alternating patches of densely vegetated blue gramma and patches of bare soil have emerged at this site in the past 8 years (Sticpewich et al., 2021). This has observed along with an overall decline in blue gamma cover, decreasing cover in shortgrass habitats by 62% since 1999 (Rondeau et al., 2016). This has been the result of severe drought and increased temperatures that have been recorded over the past 15 years at Chico Basin Ranch (Sticpewich et al., 2021). This decline in blue gamma cover has major implications for the future of the local ecosystem and economy. The potential for catastrophic population collapse would

greatly affect the ranching industry in the area, as blue gramma is one of the most nutritionally dense food-sources for the cows of Chico Basin Ranch (Rondeau et al., 2016).

Cross et al. (2022) observed a positive feedback loop at this site, which correlated local air temperature to vegetation density. This study found that patches of densely vegetated blue gramma were cooler than areas of bare soil by approximately 4.8ºC. These findings indicate the evapotranspiration of blue gramma cools local air temperature to a condition that supports growth, whereas areas without vegetation are too hot for vegetation to grow.